

# New scalings in nuclear fragmentation

E. Bonnet,<sup>1,2</sup> B. Borderie,<sup>2</sup> N. Le Neindre,<sup>2,3</sup> Ad. R. Raduta,<sup>2,4</sup> M. F. Rivet,<sup>2</sup> R. Bougault,<sup>3</sup> A. Chbihi,<sup>1</sup> J.D. Frankland,<sup>1</sup> E. Galichet,<sup>2,5</sup> F. Gagnon-Moisan,<sup>2,6</sup> D. Guinet,<sup>7</sup> P. Lantesse,<sup>7</sup> J. Lukasik,<sup>8</sup> P. Marini,<sup>2,1</sup> M. Pârlog,<sup>3,4</sup> E. Rosato,<sup>9</sup> R. Roy,<sup>6</sup> G. Spadaccini,<sup>9</sup> M. Vigilante,<sup>9</sup> J.P. Wieleccko,<sup>1</sup> and B. Zwieglinski<sup>10</sup>

(INDRA and ALADIN Collaborations)

<sup>1</sup>GANIL, (DSM-CEA/CNRS/IN2P3), F-14076 Caen cedex, France

<sup>2</sup>Institut de Physique Nucléaire, CNRS/IN2P3, Université Paris-Sud 11, F-91406 Orsay cedex, France

<sup>3</sup>LPC, CNRS/IN2P3, Ensicaen, Université de Caen, F-14050 Caen cedex, France

<sup>4</sup>National Institute for Physics and Nuclear Engineering, RO-76900 Bucharest-Magurele, Romania

<sup>5</sup>Conservatoire National des Arts et Métiers, F-75141 Paris cedex 03, France

<sup>6</sup>Laboratoire de Physique Nucléaire, Département de Physique,

de Génie Physique et d'Optique, Université Laval, Québec, Canada G1K 7P4

<sup>7</sup>Institut de Physique Nucléaire, CNRS/IN2P3, Université Claude Bernard Lyon 1, F-69622 Villeurbanne cedex, France

<sup>8</sup>Institute of Nuclear Physics IFJ-PAN, PL-31342 Kraków, Poland

<sup>9</sup>Dipartimento di Scienze Fisiche e Sezione INFN,

Università di Napoli "Federico II", I-80126 Napoli, Italy

<sup>10</sup>The Andrzej Soltan Institute for Nuclear Studies, PL-00681 Warsaw, Poland

(Dated: October 31, 2018)

Fragment partitions of fragmenting hot nuclei produced in central and semiperipheral collisions have been compared in the excitation energy region 4-10 MeV per nucleon where radial collective expansion takes place. It is shown that, for a given total excitation energy per nucleon, the amount of radial collective energy fixes the mean fragment multiplicity. It is also shown that, at a given total excitation energy per nucleon, the different properties of fragment partitions are completely determined by the reduced fragment multiplicity (fragment multiplicity normalized to the source size). Freeze-out volumes seem to play a role in the scalings observed.

PACS numbers: 25.70.-z Low and intermediate energy heavy-ion reactions ; 25.70.Pq Multifragment emission and correlations

The process of the total disintegration of a nucleus accompanied by a copious production of nuclear fragments, termed multifragmentation, was discovered more than forty years ago [1]. However, tremendous progress in the understanding of multifragmentation came during the last fifteen years with the advent of powerful  $4\pi$  detectors [2–4]. From the theoretical side, the equation of state describing nuclear matter, similar to the van der Waals equation for classical fluids, foresees the existence of a liquid-gas type phase transition and multifragmentation was long assimilated to this transition. In the last ten years the general theory of first order phase transition in finite systems was strongly progressing [5–7]. Today a rather coherent picture has been reached which is related to the experimental observation of different phase transition signatures for hot multifragmenting nuclei [4, 8–15]. The region of phase coexistence was identified in a semi-quantitative way (3 to 10 A MeV excitation energy and 0.7 to 0.2 times the normal density) and it is experimentally observed that fluctuations (configurational energy and charge of the heaviest fragment) are large and even maximum in the middle of this region for multifragmenting nuclei produced in semiperipheral collisions [16]. Such large fluctuations seem to correlate points at a distance comparable to the linear size of the system and can therefore have an effect, in the coexistence region, similar to a diverging correlation length in an infinite system at

the critical point [16–18]. Consequently one can expect to reveal new specific scalings related to a first order phase transition for finite systems. To do that, in this Letter, we compare, with the help of the reduced fragment multiplicity, the fragment partition properties of fragmenting hot nuclei produced in central and semiperipheral collisions.

The experiments were performed with the  $4\pi$  multidetector for charged reaction products INDRA [20]. For central collisions, beams of  $^{129}\text{Xe}$ , accelerated by the GANIL accelerator in Caen, France, at five incident energies: 25, 32, 39, 45 and 50 MeV/nucleon, bombarded a thin target of natural tin ( $350 \mu\text{g}/\text{cm}^2$ ) and hot quasi-fused (QF) nuclei/sources with Z around 70-100 could be selected [12]. Hot nuclei with lower Z around 60-70 (quasi-projectile, QP, sources) were obtained in semiperipheral Au+Au collisions at 80 and 100 MeV/nucleon incident energies at the SIS heavy ion synchrotron at the GSI facility in Darmstadt, Germany [21]. In this experiment the  $^{197}\text{Au}$  beam was impinging on a  $2 \text{ mg}/\text{cm}^2$  thick target. For both experiments, Z identification was obtained over the whole range of fragments produced and the energy calibration was achieved with an accuracy of 4%. Further details can be found in [22–24].

The procedures used to select the studied nuclei/sources are the following. First of all poorly-measured events were rejected by requiring the detection

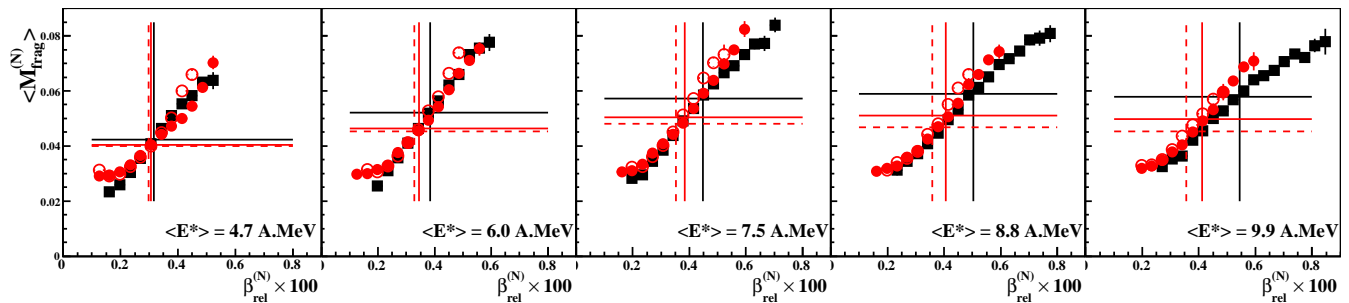


FIG. 1: (color online) Evolution of the average fragment multiplicity normalized to the source charge/size  $\langle M_{frag}^{(N)} \rangle = \langle M_{frag}/Z_s \rangle$  as a function of the relative velocity of fragments,  $\beta_{rel}^{(N)}$ , (see text) for different total excitation energy per nucleon of the sources. Full squares, open and full circles stand respectively for QF sources and QP sources produced at 80 and 100 MeV/nucleon incident energies. Crosses correspond to the mean values of the considered samples for QF (black) and QP (grey dashed-80 MeV/nucleon and full-100 MeV/nucleon) samples, see text.

$E_{inc}$ (MeV/nucleon)	25	32	39	45	50
$\langle E^* \rangle$ (A.MeV)	4.7	6.0	7.5	8.8	9.9
$\sigma_{E^*}$ (A.MeV)	0.7	0.8	1.0	1.1	1.3

TABLE I: Selected excitation energy bins for the comparison between QF and QP sources. The five columns stand for the five bombarding energies for producing QF sources (first line). Second and third lines indicate the mean value and root mean square of excitation energy ( $E^*$ ) distributions for QF sources. For comparisons, QF and QP events are limited to those with excitation energies defined as  $|E^* - \langle E^* \rangle| \leq 0.3 \sigma_{E^*}$ .

of at least 80% of the charge of the initial system (projectile plus target for QF sources, projectile only for QP sources). Then compact sources were selected by using topology selectors in velocity space. For QF sources the constraint of large flow angle ( $\geq 60^\circ$ ) calculated with the kinetic energy tensor for fragments ( $Z \geq 5$ ) in the center of mass of the reaction was imposed (for details see [12]). For QP sources it was done by imposing a maximum value (2/3 of the QP velocity) of the mean relative velocity between fragments emitted in the forward hemisphere of the center of mass (see Eqs.(1),(2) and [19] for details). A constant QP size, within 10%, was additionally required. Note that for QP sources fission events were removed [25]. Further information concerning selections and light charged particles associated to sources can be found in [19]. The following step consists in the evaluation of the total excitation energy of the different sources. The calorimetric method [26] was used event by event. Neutrons are not detected but their multiplicity is estimated from the difference between the mass of the source and the sum of the masses attributed to the detected charged products. The source is assumed to have the same  $N/Z$  ratio as the initial system. Hypotheses which have been made for QF sources are the following: a level density parameter equal to  $A/10$ , the average ki-

netic energy of neutrons equal to their emitting source temperature and the Evaporation Attractor Line formula ( $A=Z(2.072+2.32 \times 10^{-3}Z)$ ) [27] used to calculate fragment masses. EAL is especially well-adapted when heavy fragments ( $Z > 20$ ) result from the deexcitation of neutron deficient sources. For QP sources the hypotheses are identical except for calculated fragment masses for which we use the formula ( $A=Z(2.045+3.57 \times 10^{-3}Z)$ ) [27], better adapted for excited nuclei close to the beta-stability valley. Note that, compared to the EAL formula, differences appear only for masses associated to  $Z$  greater than 40.

In the following, we will use as main sorting parameter the total excitation energy per nucleon,  $E^*$ , to compare fragment properties of both QF and QP sources. Excitation energy bins of compared samples have been fixed by values (mean and  $\sigma$ ) calculated for QF sources at the five incident energies (see Table I). Only the mean values are reported in the panels of figures.

We suppose that fragment velocities, in their source frame, are the results of the composition of three components: a randomly-directed thermal contribution, a Coulomb contribution dependent on the fragment charges and source sizes, and a radial collective energy. To evaluate the radial collective energy involved in the de-excitation of the different sources the mean relative velocity between fragments

$$\beta_{rel} = \frac{2}{M_{frag}(M_{frag} - 1)} \sum_{i < j} |\beta^{(ij)}| \quad (1)$$

$$\beta^{(ij)} = \vec{\beta}^{(i)} - \vec{\beta}^{(j)} \quad (2)$$

is used, which is independent of the reference frame. Only events or subevents (for QP sources) with fragment multiplicities  $M_{frag}$  greater than one are considered. It was shown in [19] that this observable is a good measure of the amount of radial collective energy. The thermal component of fragment velocities has a negligible contribution

to their mean relative velocity, while increasing the size of fluctuations. The effect of the Coulomb contribution is removed by using a simple normalization

$$\beta_{rel}^{(N)} = \frac{\beta_{rel}}{\sqrt{\langle Z \rangle (Z_s - \langle Z \rangle)}} \quad (3)$$

which takes into account, event by event, the Coulomb influence of the mean fragment charge ( $\langle Z \rangle$ ) on the complement of the source charge ( $Z_s - \langle Z \rangle$ ).

We first look at the most global observable: the mean fragment multiplicity. Figure 1 shows that, for a given total excitation energy per nucleon, the mean fragment multiplicity normalized to the source charge/size  $\langle M_{frag}^{(N)} \rangle = \langle M_{frag} / Z_s \rangle$  is strongly correlated with the amount of radial collective expansion, as measured by  $\beta_{rel}^{(N)}$ . Crosses correspond to mean values for each type of source. Depending on the source type the relative contributions of radial collective energy (thermal pressure and compression-expansion cycle) strongly differ [19] but in all cases  $\beta_{rel}^{(N)}$ , representative of the total collective energy, fixes the normalized mean fragment multiplicity. Note that for the largest  $\beta_{rel}^{(N)}$  values (above 0.006) reached only at the higher excitation energies for QF sources, normalized fragment multiplicities increase more slowly. In that case the average size of fragments decreases and a larger fraction of them have a charge below our fragment limit  $Z=5$ .

One can now go a step further and study the properties of fragment partitions (total charge bound in fragments, heaviest fragment, asymmetry in charge of fragments) associated to the different values of the fragment multiplicity distributions. To do that, and to be able to compare QF and QP sources, we introduce a new variable the reduced fragment multiplicity  $M_{frag} / \langle Z_s \rangle$ . It is built from Fig. 2 (left side) which shows the evolutions of the mean source size with the different values,  $M_{frag}$ , of the fragment multiplicity distributions for the different excitation energies per nucleon. Figure 2 (right side) shows the evolution with the reduced fragment multiplicity of the total charge bound in fragments normalized to the source charge/size,  $Z_{frag}^{(N)}$ , for the different excitation energies per nucleon. We observe that the mean values of  $Z_{frag}^{(N)}$  are independent of the source type. On the left side of Fig.3 average values of the heaviest fragment charge,  $Z_1$ , are reported: values for QP and QF sources follow exactly the same evolution. The independence of  $Z_1$  on the system size was already observed and is valid as long as the total system or projectile mass is above 190 [4, 28]. Finally the division of the charge among the other fragments is investigated using the generalized charge asymmetry of the fragment partitions,

$$A_Z = \frac{1}{\sqrt{M_{frag} - 1}} \frac{\sigma_Z}{\langle Z \rangle} \quad (4)$$

which was introduced in [19]. One can re-calculate the generalized asymmetry by removing  $Z_1$  from partitions

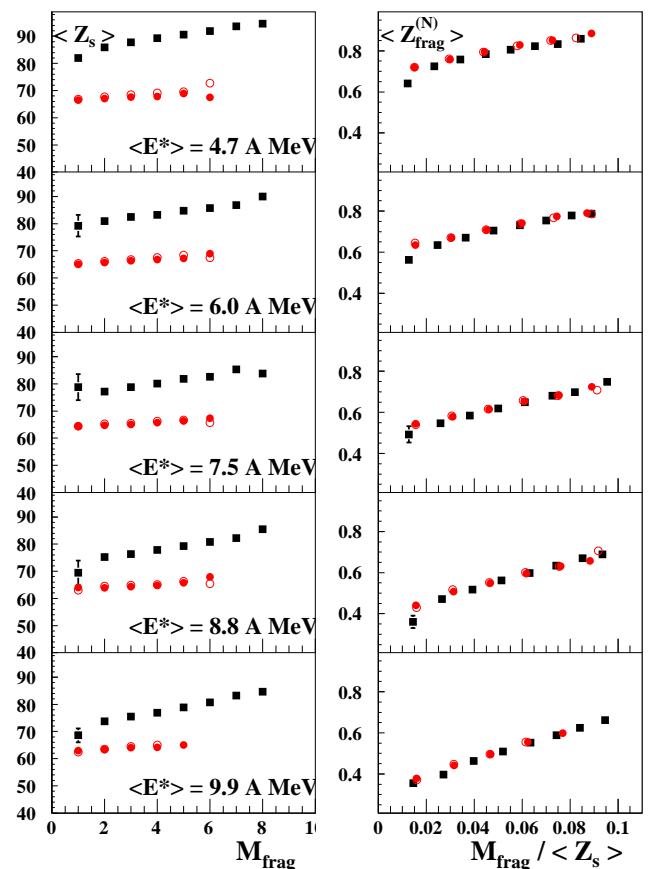


FIG. 2: (color online) Left side refers to mean values of source charges as a function of fragment multiplicity for different total excitation energy per nucleon of the sources. Right side shows the evolution of the total charge bound in fragments normalized to the source charge/size,  $Z_{frag}^{(N)}$ , as a function of the reduced fragment multiplicity  $M_{frag} / \langle Z_s \rangle$  for the same total excitation energies. Full squares, open and full circles stand respectively for QF sources and QP sources produced at 80 and 100 MeV/nucleon incident energies.

with at least 3 fragments noted  $A_Z \setminus \{Z_1\}$ . The results are displayed in Fig. 3 (right side). They follow a linear behavior and do not depend on the source type at a given total excitation energy per nucleon.

To summarize, we have shown in this Letter new results independent of the mechanism of production of hot fragmenting nuclei. First, at a given total excitation energy per nucleon, the amount of the radial collective energy fixes the mean fragment multiplicity normalized to the charge/size of the fragmenting hot nucleus; we recall that in the multifragmentation regime (3-10 A MeV) the radial collective energy is limited to at most 20% of the total excitation energies involved [19]. And secondly, the properties of fragment partitions are completely determined by the reduced fragment multiplicity. What is the possible origin of the scalings observed? To, at least, give a direction to follow for future studies, we

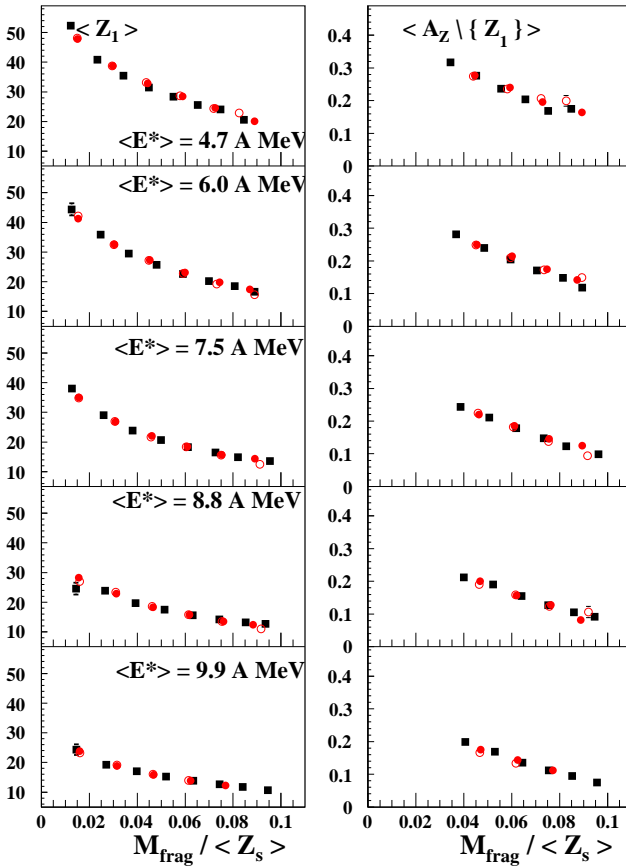


FIG. 3: (color online) Left and right sides refer respectively to the mean charge of the heaviest fragment of partitions,  $\langle Z_1 \rangle$ , and to the generalized asymmetry in charge of the fragment partitions without the heaviest one,  $A_Z \setminus \{Z_1\}$ , (see text) as a function of the reduced fragment multiplicity,  $M_{frag} / \langle Z_s \rangle$ , for different total excitation energy per nucleon of the sources. Full squares, open and full circles stand respectively for QF sources and QP sources produced at 80 and 100 MeV/nucleon incident energies.

have checked to what extent fragment partition scalings are compatible with statistical multifragmentation models with cluster degrees of freedom. The standard version of the Microcanonical Multifragmentation Model (MMM) [29, 30] was used. Inputs were the average A and Z of QF and QP sources at the different total excitation energies per nucleon. Contributions of radial collective energy to the total excitation energy were taken from [19]. We do obtain fragment partition scalings if and only if the freeze-out volume of the QF sources increases monotonically with the total excitation energy from 2.7 to 5.7  $V_0$  and the freeze-out volume of the QP sources is kept fixed at the intermediate value of 3.5  $V_0$ ;  $V_0$  would correspond to the volume of the source at normal density. However the agreement between MMM results and the present observed scalings is partial: a rather fair agree-

ment for  $Z_{frag}^{(N)}$  and  $Z_1$  and a systematic underestimation for the fragment asymmetry without  $Z_1$ . We recall that in MMM the radial collective energy is decoupled from the break-up thermodynamics and fragment formation. Clearly dynamical approaches, which contain the coupling between thermal and collective expansion effects to produce fragments [31], must be compared to those data.

- 
- [1] Y. F. Gagarin et al., Sov. J. Nucl. Phys. 11 (1970) 698.
  - [2] P. Chomaz et al. (eds.) vol. 30 of *Eur. Phys. J. A*, Springer, 2006.
  - [3] V. E. Viola et al., Phys. Rep. 434 (2006) 1.
  - [4] B. Borderie et al., Prog. Part. Nucl. Phys. 61 (2008) 551.
  - [5] D. H. E. Gross, Microcanonical Thermodynamics - Phase Transitions in "small" systems, World Scientific, Singapore, 2001.
  - [6] F. Gulminelli et al., Nucl. Phys. A 734 (2004) 581.
  - [7] P. Chomaz et al., Phys. Rep. 389 (2004) 263.
  - [8] J. Pochodzalla et al. (ALADIN Collaboration), Phys. Rev. Lett. 75 (1995) 1040.
  - [9] M. D'Agostino et al., Phys. Lett. B 473 (2000) 219.
  - [10] B. Borderie et al. (INDRA Collaboration), Phys. Rev. Lett. 86 (2001) 3252.
  - [11] J. B. Natowitz et al., Phys. Rev. C 65 (2002) 034618.
  - [12] G. Tăbăcaru et al., Eur. Phys. J. A 18 (2003) 103.
  - [13] M. D'Agostino et al., Nucl. Phys. A 734 (2004) 512.
  - [14] M. Bruno et al., Nucl. Phys. A 807 (2008) 48.
  - [15] E. Bonnet et al. (INDRA Collaboration), Phys. Rev. Lett. 103 (2009) 072701.
  - [16] N. Le Neindre et al. (INDRA and ALADIN collaborations), Nucl. Phys. A 795 (2007) 47.
  - [17] F. Gulminelli et al., Phys. Rev. Lett. 82 (1999) 1402.
  - [18] J. M. Yeomans, Statistical Mechanics of Phase Transitions, Oxford University Press, Oxford, 1992.
  - [19] E. Bonnet et al. (INDRA and ALADIN Collaborations), Nucl. Phys. A 816 (2009) 1.
  - [20] J. Pouthas et al., Nucl. Instr. and Meth. in Phys. Res. A 357 (1995) 418.
  - [21] J. Lukasik et al. (INDRA and ALADIN collaborations), Phys. Lett. B 566 (2003) 76.
  - [22] G. Tăbăcaru et al. (INDRA Collaboration), Nucl. Instr. and Meth. in Phys. Res. A 428 (1999) 379.
  - [23] M. Pârlog et al. (INDRA Collaboration), Nucl. Instr. and Meth. in Phys. Res. A 482 (2002) 693.
  - [24] A. Trzciński et al. (INDRA and ALADIN collaborations), Nucl. Inst. Meth. A501 (2003) 367.
  - [25] M. Pichon et al. (INDRA and ALADIN collaborations), Nucl. Phys. A 779 (2006) 267.
  - [26] V. E. Viola et al., P. Chomaz et al. (eds.) Dynamics and Thermodynamics with nuclear degrees of freedom, Springer, 2006, vol. 30 of *Eur. Phys. J. A*, 215–226.
  - [27] R. J. Charity, Phys. Rev. C 58 (1998) 1073.
  - [28] M. F. Rivet et al. (INDRA Collaboration), Phys. Lett. B 430 (1998) 217.
  - [29] A. H. Raduta et al., Phys. Rev. C 55 (1997) 1344.
  - [30] A. H. Raduta et al., Phys. Rev. C 65 (2002) 054610.
  - [31] J. Rizzo et al., Phys. Rev. C 76 (2007) 024611.